



Publication Year	2022
Acceptance in OA	2024-03-01T15:38:51Z
Title	Calibration of the IXPE Focal Plane X-Ray Polarimeters to Polarized Radiation
Authors	DI MARCO, Alessandro, FABIANI, Sergio, LA MONACA, Fabio, MULERI, FABIO, RANKIN, John, SOFFITTA, PAOLO, XIE, FEI, AMICI, FABRIZIO, ATTINA', Primo, BACHETTI, Matteo, Baldini, Luca, Barbanera, Mattia, Baumgartner, Wayne, Bellazzini, Ronaldo, Borotto, Fabio, Brez, Alessandro, BRIENZA, Daniele, Caporale, Ciro, Cardelli, Claudia, Carpentiero, Rita, Castellano, Simone, Castronuovo, Marco, Cavalli, Luca, Cavazzuti, Elisabetta, Ceccanti, Marco, CENTRONE, Mauro, Citraro, Saverio, COSTA, ENRICO, D'Alba, Elisa, D'AMICO, Fabio, DEL MONTE, Ettore, DI COSIMO, SERGIO, Di Lalla, Niccolò, DI PERSIO, GIUSEPPE, Donnarumma, Immacolata, EVANGELISTA, YURI, FERRAZZOLI, RICCARDO, Latronico, Luca, LEFEVRE, CARLO, LOFFREDO, Pasqualino, Lorenzi, Paolo, Lucchesi, Leonardo, Magazzù, Carlo, Magazzù, Guido, Maldera, Simone, Manfreda, Alberto, Mangraviti, Elio, Marengo, Marco, Matt, Giorgio, Mereu, Paolo, Minuti, Massimo, MORBIDINI, Alfredo, Mosti, Federico, Nasimi, Hikmat, Negri, Barbara, NUTI, Alessio, O'Dell, Stephen L., Orsini, Leonardo, PERRI, Matteo, Pesce-Rollins, Melissa, PIAZZOLLA, RAFFAELE, Pieraccini, Stefano, PILIA, Maura, Pinchera, Michele, Profeti, Alessandro, Puccetti, Simonetta, Ramsey, Brian D., RATHEESH, AJAY, RUBINI, ALDA, SANTOLI, Francesco, Sarra, Paolo, SCALISE, Emanuele, Sciortino, Andrea, Sgrò, Carmelo, Spandre, Gloria, Tardiola, Marcello, Tennant, Allyn F., TOBIA, ANTONINO, TROIS, ALESSIO, Vimercati, Marco, Weisskopf, Martin C., Zanetti, Davide, Zanetti, Francesco
Publisher's version (DOI)	10.3847/1538-3881/ac7719
Handle	http://hdl.handle.net/20.500.12386/34855
Journal	THE ASTRONOMICAL JOURNAL
Volume	164



Calibration of the IXPE Focal Plane X-Ray Polarimeters to Polarized Radiation

Alessandro Di Marco¹, Sergio Fabiani¹, Fabio La Monaca¹, Fabio Muleri¹, John Rankin^{1,2,3}, Paolo Soffitta¹, Fei Xie¹, Fabrizio Amici¹, Primo attinà⁴, Matteo Bachetti⁵, Luca Baldini^{6,7}, Mattia Barbanera^{7,8}, Wayne Baumgartner⁹, Ronaldo Bellazzini⁷, Fabio Borotto¹⁰, Alessandro Brez⁷, Daniele Brienza¹, Ciro Caporale¹⁰, Claudia Cardelli⁷, Rita Carpentiero¹¹, Simone Castellano⁷, Marco Castronuovo¹¹, Luca Cavalli¹², Elisabetta Cavazzuti¹¹, Marco Ceccanti⁷, Mauro Centrone¹³, Saverio Citraro⁷, Enrico Costa¹, Elisa D'Alba¹², Fabio D'Amico¹⁶, Ettore Del Monte¹, Sergio Di Cosimo¹, Niccolò Di Lalla¹⁴, Giuseppe Di Persio¹, Immacolata Donnarumma¹¹, Yuri Evangelista¹, Riccardo Ferrazzoli^{1,2,3}, Luca Latronico¹⁰, Carlo Lefevre¹, Pasqualino Loffredo¹, Paolo Lorenzi¹², Leonardo Lucchesi⁷, Carlo Magazzù⁷, Guido Magazzù⁷, Simone Maldera¹⁰, Alberto Manfreda⁷, Elio Mangraviti¹², Marco Marengo¹⁰, Giorgio Matt¹⁵, Paolo Mereu¹⁰, Massimo Minuti⁷, Alfredo Morbidini¹, Federico Mosti¹⁰, Hikmat Nasimi⁷, Barbara Negri¹¹, Alessio Nuti⁷, Stephen L. O'Dell⁹, Leonardo Orsini⁷, Matteo Perri¹³, Melissa Pesce-Rollins⁷, Raffaele Piazzolla¹¹, Stefano Pieraccini¹², Maura Pilia⁵, Michele Pinchera⁷, Alessandro Profeti⁷, Simonetta Puccetti¹¹, Brian D. Ramsey⁹, Ajay Ratheesh^{1,2,3}, Alda Rubini¹, Francesco Santoli¹, Paolo Sarra¹², Emanuele Scalise¹, Andrea Sciortino¹², Carmelo Sgrò⁷, Gloria Spandre⁷, Marcello Tardiola¹², Allyn F. Tennant⁹, Antonino Tobia¹, Alessio Trois⁵, Marco Vimercati¹², Martin C. Weisskopf⁹, Davide Zanetti⁷, and Francesco Zanetti¹²

¹ INAF-IAPS, via Fosso del Cavaliere, 100, I-00133 Roma, Italy; alessandro.dimarco@inaf.it

² Università di Roma "La Sapienza", Dipartimento di Fisica, Piazzale Aldo Moro 2, I-00185 Roma, Italy

³ Università di Roma "Tor Vergata", Dipartimento di Fisica, Via della Ricerca Scientifica, 1, I-00133 Roma, Italy

⁴ INAF/Osservatorio Astrofisico di Torino, Via Osservatorio 20, Pino Torinese, I-10025 Torino, Italy

⁵ INAF-OAC, Via della Scienza 5, Selargius, I-09047 Cagliari, Italy

⁶ Università di Pisa, Dipartimento di Fisica Enrico Fermi, Largo B. Pontecorvo 3, I-56127 Pisa, Italy

⁷ INFN-Pisa, Largo B. Pontecorvo 3, I-56127 Pisa, Italy

⁸ Università di Pisa, Dipartimento di Ingegneria dell'Informazione, Via G. Caruso 16, I-56122 Pisa, Italy

⁹ NASA Marshall Space Flight Center, Huntsville, AL 35812, USA

¹⁰ INFN-Torino, Via P. Giuria, 1, I-10125 Torino, Italy

¹¹ ASI, Via del Politecnico snc, I-00133 Roma, Italy

¹² OHB Italia, Via Gallarate 150, I-20151 Milano, Italy

¹³ INAF/OAR, Via Frascati 33, Monte Porzio Catone, I-00040 Roma, Italy

¹⁴ Kavli Institute, Department of Physics and SLAC, Stanford University, Stanford, CA 94305, USA

¹⁵ Università Roma Tre, Dipartimento di Matematica e Fisica, Via della Vasca Navale 84, I-00146, Italy

Received 2022 March 7; revised 2022 April 28; accepted 2022 June 7; published 2022 August 18

Abstract

The Imaging X-ray Polarimetry Explorer (IXPE) is a NASA Small Explorer mission—in partnership with the Italian Space Agency—dedicated to X-ray polarimetry in the 2–8 keV energy band. The IXPE telescope comprises three grazing incidence mirror modules coupled to three detector units hosting each one a Gas Pixel Detector, a gas detector that allows measuring the polarization degree by using the photoelectric effect. A wide and accurate ground calibration was carried out on the IXPE Detector Units at INAF-IAPS, in Italy, where a dedicated facility was setup at this aim. In this paper, we present the results obtained from this calibration campaign to study the IXPE focal plane detector response to polarized radiation. In particular, we report on the modulation factor, which is the main parameter to estimate the sensitivity of a polarimeter.


Unified Astronomy Thesaurus concepts: X-ray astronomy (1810); Polarimetry (1278)

1. Introduction

The Imaging X-ray Polarimetry Explorer (IXPE; Weisskopf et al. 2016; Soffitta 2017; O'Dell et al. 2019; Soffitta et al. 2020; Ramsey et al. 2021; Soffitta et al. 2021; Weisskopf et al. 2021) will be the first X-ray astronomy mission fully dedicated to polarimetry; it will expand our knowledge on X-ray sources, adding polarization data to temporal, spectral, and imaging ones allowing to obtain scientifically relevant measurements from several sources (e.g., neutron stars, black holes, active Galactic nuclei, supernova remnants, etc.). Despite the importance of polarimetric information, the only available statistically significant

measurements of X-ray polarization were obtained for the Crab Nebula (Weisskopf et al. 1976, 1978) over 40 yr ago by using the crystal polarimeters aboard the Orbiting Solar Observatory 8 and recently by PolarLight (Feng et al. 2020), albeit with a much smaller significance.¹⁶

IXPE was launched on 2021 December 9th into a near-equatorial circular orbit at about 600 km altitude. The IXPE Payload comprises three X-ray telescopes, each one with a X-ray optics and one detector unit (DU) separated by a shared optical bench (boom), deployed to match the telescopes' focal length. Each DU lid has mounted on a collimator, an ions-UV filter (La Monaca et al. 2021). Each DU is equipped with a Filter and Calibration Wheel (Muleri et al. 2018; Ferrazzoli et al. 2020), the

 Original content from this work may be used under the terms of the [Creative Commons Attribution 4.0 licence](https://creativecommons.org/licenses/by/4.0/). Any further distribution of this work must maintain attribution to the author(s) and the title of the work, journal citation and DOI.

¹⁶ Recently also a low-significance measurement of polarization of Sco-X1 has been performed by PolarLight (Long et al. 2022).

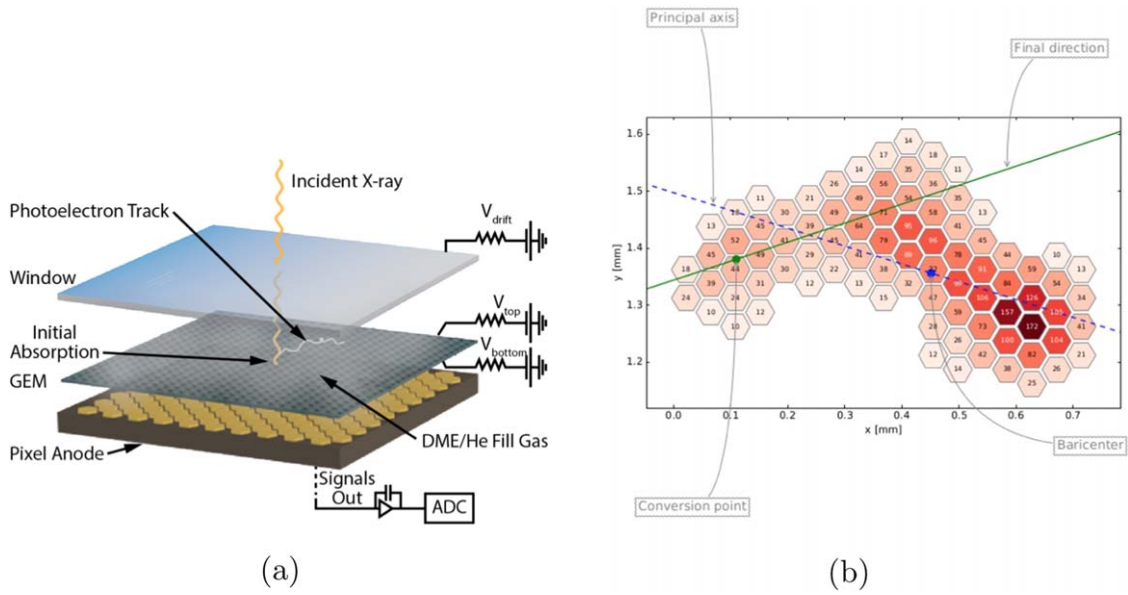


Figure 1. A schematic view of the GPD is shown on the (a) panel; the (b) panel displays an ionization track resulting from absorption of a 5.9 keV X-ray imaged onto the GPD’s pixelated anode (Sgrò, 2017).

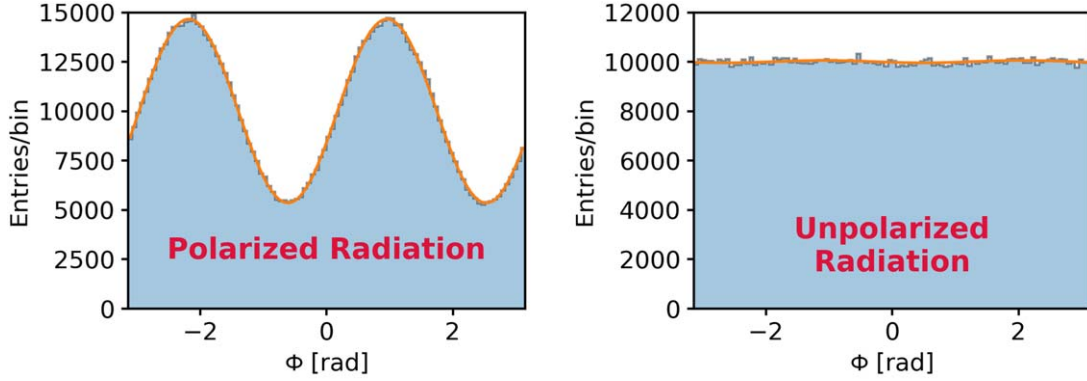


Figure 2. Distribution of photoelectrons directions (modulation curves) produced by polarized (left) and unpolarized (right) radiation at 5.89 keV (Rankin et al. 2022).

Gas Pixel Detector (GPD; Costa et al. 2001; Bellazzini et al. 2006, 2007; Baldini et al. 2021), and the Back-End Electronics (Barbanera et al. 2021), which connects to the Detector Service Unit. The whole IXPE instrument has been built by INAF-IAPS and INFN, and it is described in more detail in Soffitta et al. (2021).

The GPD was invented and developed by the IXPE Italian team, and it allows one to obtain an image of the ionization track produced by the photoelectron resulting from absorption of an X-ray in the gas cell (see Figure 1(a)). The imaged ionization tracks (see the example in Figure 1(b)) contains information on the photoelectron’s energy and direction, which is correlated with the polarization orientation of the absorbed X-ray (in case of orbital s electrons), as described by the differential cross section (Heitler 1936):

$$\frac{d\sigma}{d\Omega} = r_0^2 \frac{Z^5}{137^4} \left(\frac{mc^2}{h\nu} \right)^{7/2} \frac{4\sqrt{2} \sin^2(\theta) \cos^2(\phi)}{[1 - \beta \cos(\theta)]^4}, \quad (1)$$

where r_0 is the classical electron radius, Z the atomic number of the gas, mc^2 is the rest electron mass, $h\nu$ is the photon energy, β the fraction of electron velocity with respect to the speed of light, and θ and ϕ are the polar and azimuthal angles, respectively. Then, in a photoelectric polarimeter, the X-rays interaction

produces mainly photoelectrons with a $\cos^2(\phi)$ angular distribution. As shown in Figure 2, photoelectrons angular distribution for a polarized (left) X source show a $\cos^2(\phi)$ modulation that is not observable in the case of an unpolarized source (right). The modulation amplitude, M , of the modulation curves is proportional to the polarization degree of the source, P . To obtain P from a measured M we need a parameter, named modulation factor, μ :

$$P = \frac{M}{\mu}. \quad (2)$$

The modulation factor is a property of the detector (the most important parameter for the calculation of the sensitivity for a polarimeter) and is given by the modulation amplitude measured in the presence of a 100% polarized source.

Because IXPE is a discovery mission, standard celestial sources are not available for performing in-flight calibration for polarimetry because the few available measurements of polarization obtained in the past (Weisskopf et al. 1976, 1978; Feng et al. 2020; Long et al. 2022) cannot be used as a flight calibrator; also because the source is known to vary. Because gas detectors based on GEM can have a time-dependent response, IXPE is equipped with an on-board calibration system and a detailed ground

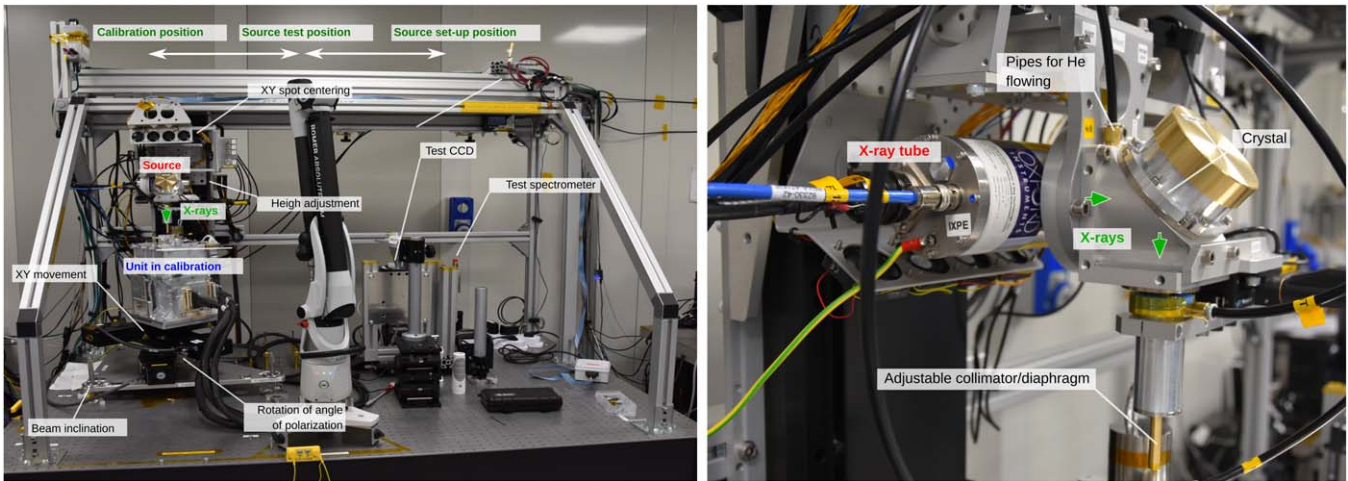


Figure 3. Left: frontal view of the ICE during a measurement with a DU-FM. Right: view of one of the polarized sources setup Muleri et al. (2021).

Table 1
List of Polarized Sources Setups Used During DU-FM Ground Calibrations Muleri et al. (2018, 2021)

Crystal	X-Ray Tube	Energy (keV)	2d (Å)	Diffraction angle (deg)	Rp/Rs	Polarization (%)
PET (002)	Continuum	2.01	8.742	45.00	0.0000	≈100.0%
InSb (111)	Mo ($L\alpha$)	2.29	7.481	46.28	0.0034	99.3%
Ge (111)	Rh ($L\alpha$)	2.70	6.532	44.73	0.0024	99.5%
Si (111)	Ag ($L\alpha$)	2.98	6.271	41.49	0.0252	95.1%
Al (111)	Ca ($K\alpha$)	3.69	4.678	45.90	0.0031	99.4%
Si (220)	Ti ($K\alpha$)	4.51	3.840	45.73	0.0023	99.5%
Si (400)	Fe ($K\alpha$)	6.40	2.716	45.51	...	≈100.0%

calibration was mandatory. At this aim, a wide calibration campaign has been performed at INAF-IAPS in Rome. During this campaign, data were acquired 24 hr per day and 7 days per week: for each DU at least 40 days of calibrations were needed. Each of the four DUs have been calibrated separately (three DU to be integrated on the payload plus a spare unit). Calibration results have also been validated by telescope calibrations, as cited in Ramsey et al. (2021) and Bongiorno et al. (2021).

In the following, the setup used during the calibration campaign is briefly presented and the used polarized sources are summarized, and a complete description is given in Muleri et al. (2021). Below, the results obtained from different methods of analysis for the modulation factor are compared, then, following the approach of Di Marco et al. (2022), the modulation factor has been widely characterized for all the IXPE DUs and results are compared with IXPE scientific requirements.

2. Experimental Setup

An extensive X-ray calibration has been performed at INAF/IAPS for all the IXPE DUs; such calibrations have been carried out with a setup named Instrument Calibration Equipment (ICE; see Figure 3), constructed with this aim in an ISO7 (10,000 class) clean room (Muleri et al. 2021). The IXPE four DU Flight Models (DU-FM), with three to be installed on the payload and one spare unit, have been calibrated with the same procedures, and the same experimental measurements have been performed. DU-FMs are named with numbers from 1 to 4 (the number 1 is the spare unit) and they were calibrated in the

order: DU-FM2, DU-FM3, DU-FM4, DU-FM1. The calibration equipment includes:

1. X-ray sources used for calibration and tests (each source emits X-ray photons at known energy and with known polarization degree and angle);
2. a control system that allows for knowing the direction of the beam, the direction of polarization for polarized sources, and its position with respect to the GPD inside the DU-FM (so it can be aligned and moved as necessary);
3. the test detectors (SDD and X-ray CCD camera) that are used to characterize the beam before DU-FM calibration and as a reference for specific measurements;
4. electrical and mechanical ground support equipment required to operate the DU-FMs.

On the ICE setup, X-ray sources are mounted on a platform that can slide in three different positions: one for setting up the source, one for testing it with test detectors, and one to calibrate the DU-FM. The stages, controlled independently, allow for aligning the source to the DU-FM and to move it with respect to the source during calibration. These stages allow controlling the geometry of the setup with a sensitivity at order of $10 \mu\text{m}$.

At INAF-IAPS both polarized and unpolarized sources are available (Muleri et al. 2021) and have been used during ground calibrations. Measurements with sources at several energies have been carried out to study the response to polarized radiation. The used polarized sources are based on commercial X-ray tubes (Oxford Series 5000 or Hamamatsu Head-on N7599 series) and Bragg diffraction at nearly 45° on a crystal, as listed in Table 1. A collimator is used with aim to

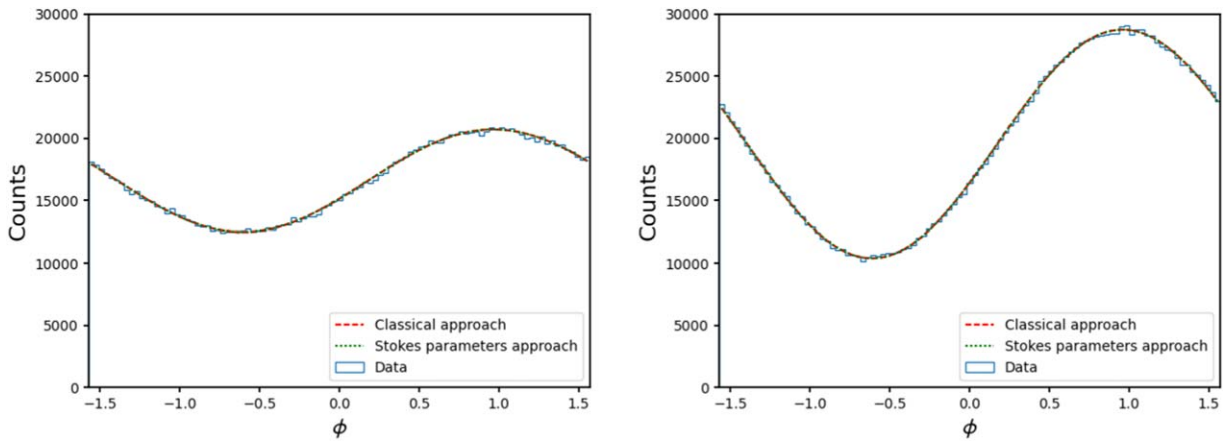


Figure 4. Example of a fit with the classical approach (see Section 3.1) and with the Stokes parameters approach (see Section 3.2) for events at 2.7 keV (left) and 6.4 keV (right). The two best-fit curves are perfectly overimposed.

obtain a beam with a well-defined and measurable direction and polarization angle and to select a portion of the diffracted and diverging beam, as shown in Figure 3 (right). A nearly flat illumination over a region is obtained translating the DU continuously on a plane perpendicular to the source beam during measurement, the algorithm used is the same as the one proposed for dithering the IXPE satellite pointing; typically, the measurement with nearly 100% polarized X-ray sources are repeated at five different polarization angles to verify that modulation factor is independent on the polarization angle as expected; moreover two of them are rotated 90° relative to each other to allow an estimate of systematic effects. Analyzed data sets comprise:

1. Polarized flat field (PolFF) at seven energies (2.01, 2.29, 2.70, 2.98, 3.69, 4.51, and 6.40 keV). These sources are monochromatic for all practical purposes and produced by a spot that is moved to illuminate a central circular area with 7 mm radius. With the flat field, a measurement covering the whole sensitive area of the detector is intended. The rotation of the DU, named ϵ_1 , is the same at all energies and it corresponds to have an expected polarization angle value of $\simeq 55^\circ$.
2. Polarized deep flat field (PolDFF) at seven energies, same sources used for PolFFs, where the spot is moved on a circular area at the center with 3.25 mm radius to collect more events per cm^2 in a shorter time. With the deep flat field, a measurement covering a smaller region on the sensitive area of the detector is intended, but with an high count rate. PolDFF are repeated at different polarization angles and the number of measurements depended on the source counting rate (sources at 2.01 and 3.69 keV having lower rates were carried out only to an angle in the DU-FM frame $\epsilon_2 = -35^\circ$, the other ones having higher rate at four angles $\epsilon_2 = 32.5^\circ$, $\epsilon_3 = 10^\circ$, $\epsilon_4 = -12.5^\circ$, and $\epsilon_5 = -35^\circ$).

The analysis in the following are performed: (i) to verify the polarimetric response uniformity of the detectors studying the FF data; (ii) after uniformity confirmation, to obtain the most sensitive estimation of the modulation factor, analyses are performed in a circular centered region with radius 3.0 mm, which is the largest region illuminated at every energy and angle during ground calibration with polarized sources.

3. Analysis Method

In literature, several methods to estimate the polarization degree and angle from data have been proposed. In the following, we recall three of them: (i) the classical one based on modulation amplitude estimation from modulation curves fit; (ii) Stokes parameters estimation from modulation curves fit Strohmayer & Kallman (2013); (iii) Stokes parameters estimation based on an unbinned event-by-event approach Kislat et al. (2015). The three methods have been applied to the same data set obtaining every time the same result, in the following they are shortly presented and applied, as an example, to data acquired with the DU-FM2 in the presence of a 100% polarized source at 2.7 keV and 6.4 keV as representative cases at low and high energy in the IXPE band.

3.1. “Classical” Approach

From Equation (1) and Figure 2–left, it is evident that the modulation curve, in presence of a polarized radiation, follows a $\cos^2 \phi$ distribution. The classical approach to obtain polarimetric information consists in fitting this distribution with the function:

$$\mathcal{M}(\phi) = A + B \cos^2(\phi - \phi_0), \quad (3)$$

from which the modulation is derived:

$$M = \frac{\mathcal{M}_{\max} - \mathcal{M}_{\min}}{\mathcal{M}_{\max} + \mathcal{M}_{\min}} = \frac{B}{2A + B}. \quad (4)$$

In this approach, the polarization angle is given directly by the fit as ϕ_0 and the polarization degree is given by:

$$P = \frac{1}{\mu} \frac{B}{2A + B}. \quad (5)$$

In Figure 4 the modulation curves at 2.7 keV (left) and 6.4 keV (right) are shown superimposed to the best-fit curves from this method (red-dashed lines). The obtained value for the modulation amplitude is reported in Table 2.

3.2. Binned Stokes Parameters Approach

An alternative approach consists in using Stokes parameters as described in Strohmayer & Kallman (2013). The polarization

Table 2
Modulation Factor and Polarization Angle Measured, for the Same Data at 2.7 keV and 6.4 keV, Using the Three Different Analysis Methods

Energy	Parameter	Classical Approach	Stokes Parameters	Event-by-event
2.7 keV	μ	$(24.80 \pm 0.14)\%$	$(24.796 \pm 0.084)\%$	$(24.81 \pm 0.11)\%$
	ϕ	$-(34.67 \pm 0.17)^\circ$	$-(34.67 \pm 0.10)^\circ$	$-(34.69 \pm 0.13)^\circ$
6.4 keV	μ	$(46.90 \pm 0.11)\%$	$(46.896 \pm 0.067)\%$	$(46.92 \pm 0.10)\%$
	ϕ	$-(34.990 \pm 0.074)^\circ$	$-(34.990 \pm 0.045)^\circ$	$-(34.989 \pm 0.062)^\circ$

degree as a function of the Stokes parameters is:

$$P = \frac{\sqrt{U^2 + Q^2}}{\mu I}, \quad (6)$$

thus for a 100% linearly polarized beam $I = \sqrt{U^2 + Q^2}$. It is convenient to use the normalized Stokes parameters, $q = Q/I$ and $u = U/I$, therefore the degree of polarization and the direction are:

$$P = \frac{\sqrt{q^2 + u^2}}{\mu}$$

$$\phi_0 = \frac{1}{2} \arctan\left(\frac{u}{q}\right). \quad (7)$$

In this approach, proposed in Strohmayer & Kallman (2013), modulation curves can be fitted with the function:

$$\mathcal{M}(\phi) = I + Q \cos(2\phi) + U \sin(2\phi), \quad (8)$$

allowing us to obtain the Stokes parameters directly from the fit. In Figure 4 the best-fit curves are shown in green-dotted lines, the modulation amplitude and phase are reported in Table 2.

3.3. Unbinned Stokes Parameters Approach

For each detected event, IXPE DUs provide the photoelectron emission direction ϕ_k ; this allows an estimate for each one of them the Stokes parameters following the approach proposed by Kislat et al. (2015):

$$\begin{aligned} i_k &= 1 \\ q_k &= 2 \cos(2\phi_k) \\ u_k &= 2 \sin(2\phi_k). \end{aligned} \quad (9)$$

From these unbinned Stokes parameters, it is possible to determine the ones for an observation of N events:

$$\begin{aligned} I &= \sum_N i_k = N \\ Q &= \sum_N q_k = Nq \\ U &= \sum_N u_k = Nu \end{aligned} \quad (10)$$

with associated uncertainties (in case of small polarization degree):

$$\begin{aligned} \sigma_I &= \sqrt{N} \\ \sigma_q &\simeq \sigma_u \simeq \sqrt{\frac{2}{N-1}}. \end{aligned}$$

The polarization degree and angle can be derived from Equations (7). In this approach there is not a fit, but only a numerical estimation that has been reported in Table 2.

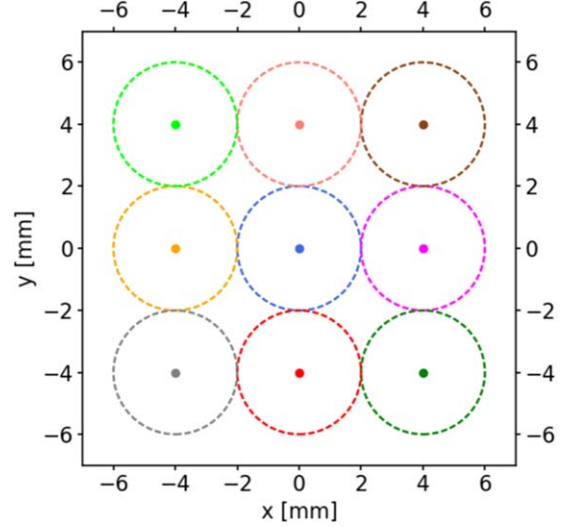


Figure 5. Independent regions in which the modulation factor is evaluated.

3.4. Adopted Analysis Approach

In Table 2 the modulation factor and the polarization angle from the three methods are compared, and they give rise to compatible values for both modulation factor and polarization angle. Stokes parameters have the great advantage of being handled as fluxes with full poissonian statistics. As an example, this allows decoupling systematic effects in polarization measurements. Moreover an unbinned analysis allows for obtaining estimations also from a low number of events and to apply a weighted analysis as described in Di Marco et al. (2022). Moreover, a polarimeter can suffer from a systematic named spurious modulation, i.e., the presence of a small modulation due to the instrument, also present when unpolarized sources are observed. This effect can be calibrated and subtracted to correct the polarization degree of the source following a correction algorithm as the one described in Rankin et al. (2022).

3.4.1. Spurious Modulation Subtraction

Two existing approaches based on the use of Stokes parameters can be applied to disentangle the spurious component from the source. The first approach decouples the two measurements acquired with the detector rotated of an angle $\epsilon_2 - \epsilon_1 = \Delta\epsilon = 90^\circ$. Calling $(q_{\text{spurious}}, u_{\text{spurious}})$ and $(q_{\text{source}}, u_{\text{source}})$ the Stokes parameters for the instrument response due to spurious effects and the source, respectively, the Stokes parameter q (or u) measured at the first and second angles read:

$$q_1 = q_{\text{spurious}}(\epsilon_1) + q_{\text{source}}(\epsilon_1) \quad (11)$$

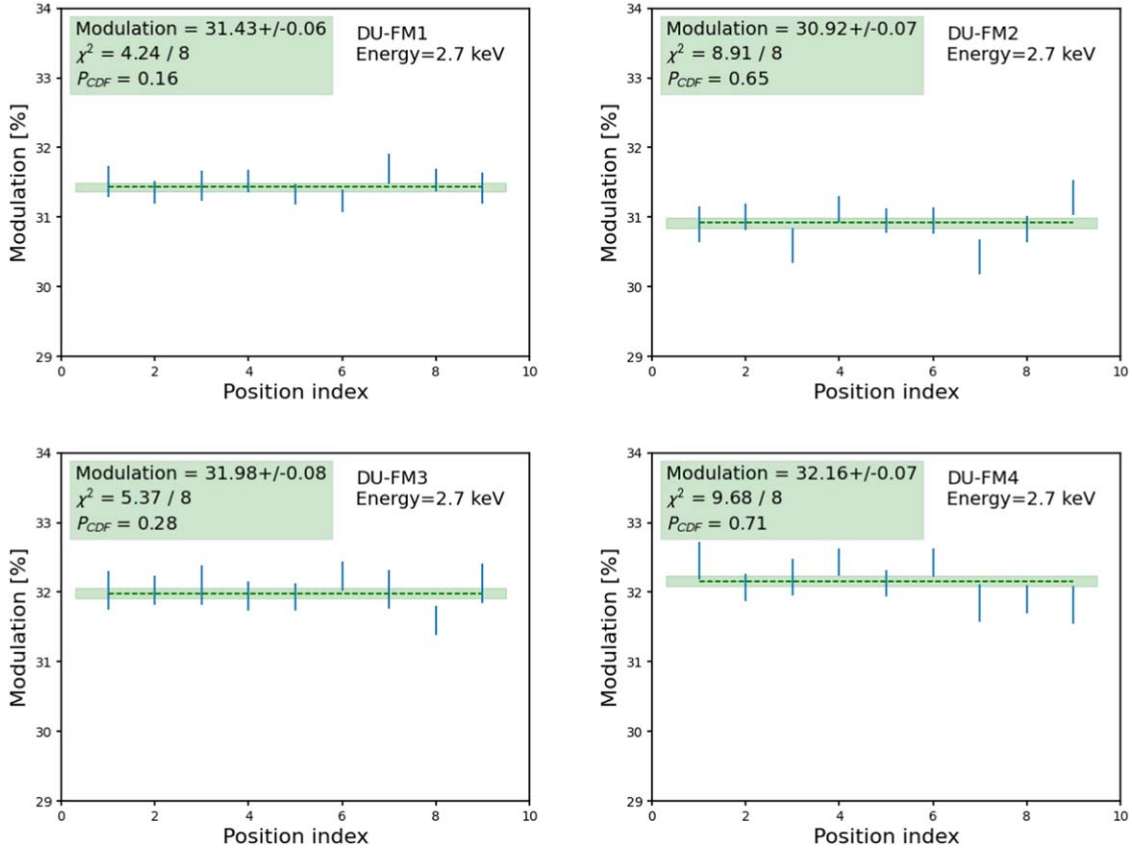


Figure 6. Modulation factor measured at 2.98 keV in nine different spots of radius 2 mm with the DU-FM1 (top left), DU-FM2 (top right), DU-FM3 (bottom left), and DU-FM4 (bottom right).

$$\begin{aligned}
 q_2 &= q_{\text{spurious}}(\epsilon_2) + q_{\text{source}}(\epsilon_2) = q_{\text{spurious}}(\epsilon_1 + 90^\circ) \\
 &\quad + q_{\text{source}}(\epsilon_1 + 90^\circ) \\
 &= q_{\text{spurious}}(\epsilon_1) - q_{\text{source}}(\epsilon_1)
 \end{aligned} \tag{12}$$

and then

$$\begin{cases} q_{\text{spurious}} = \frac{q_1 + q_2}{2} \\ q_{\text{source}} = \frac{q_1 - q_2}{2} \end{cases} \tag{13}$$

A second approach is based on calibration maps, obtained from ground measurements. For each observed event in a given GPD pixel with coordinates (x_k, y_k) and energy E_k , it is possible to subtract the spurious modulation value as explained in Rankin et al. (2022):

$$\begin{aligned}
 i_{\text{cal}} &= i_k \\
 q_{\text{cal}} &= q_k - q_{\text{sm}}(x_k, y_k, E_k) \\
 u_{\text{cal}} &= u_k - u_{\text{sm}}(x_k, y_k, E_k).
 \end{aligned} \tag{14}$$

3.4.2. Modulation Factor Estimation

In the past, GPD data analyses have been carried out by applying a selection of the events named “standard cuts” (Muleri et al. 2016; Di Marco et al. 2022), where about 20% of the events are removed. The selection is applied in two steps: (i) remove events with energy values outside $\pm 3\sigma$ from the peak centroid; (ii) remaining tracks are ordered for “elongation”

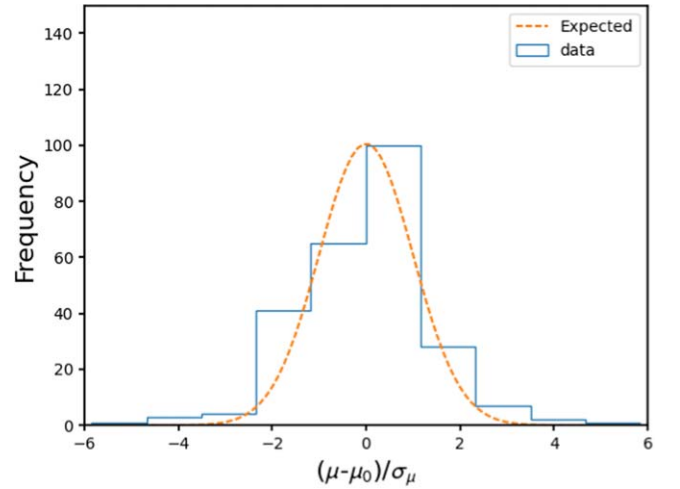


Figure 7. Distribution of the number of standard deviation, σ_{μ_i} , between the best-fit mean value on all the 9 regions of the data set (μ_0) and the single measured modulation factor (μ_i) for every energy and DU: $(\mu_i - \mu_0)/\sigma_{\mu_i}$. In dashed-orange the expected normal distribution is shown.

(which is the ratio between the track length and track width; for more details see Di Marco et al. 2022), the ones with lower-elongation are removed to reach a threshold that allows for removing 20% of the initial events, including the ones removed at the step (i). This approach cannot be applied to astronomical sources that are nonmonochromatic, thus a new approach to obtain an optimal sensitivity has been proposed in

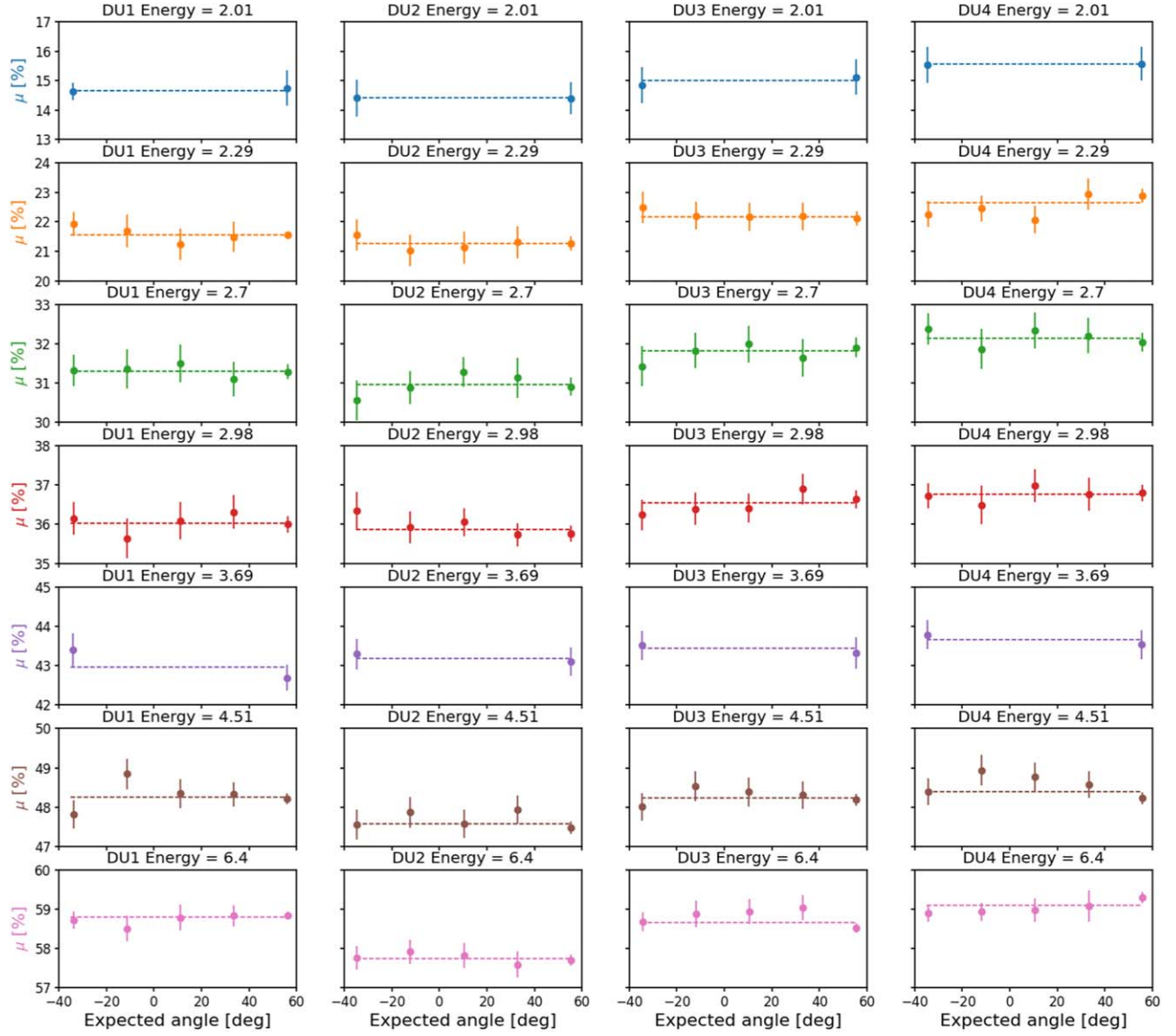


Figure 8. Modulation factor as a function of the expected polarization angle for the four DUs. Dashed lines represent the modulation factor mean values.

Di Marco et al. (2022) consisting in applying for each event an optimal weight, w_i , to the Stokes parameters:

$$\begin{aligned}
 I &= \sum_i w_i \\
 Q &= \sum_i 2w_i \sin(2\phi_i) \\
 U &= \sum_i 2w_i \cos(2\phi_i)
 \end{aligned} \quad (15)$$

where $w_i = \alpha^{0.75}$ with α given by the track ellipticity Di Marco et al. (2022). In the following, the weighted approach is applied after selection of events in a circular centered region with radius 3.0 mm.

4. Calibration of Response to Polarization

In this section, we present the analysis of the response to polarized sources for the IXPE DUs during ground calibrations.

4.1. Uniformity of Polarimetric Response

During ground calibrations, the X-ray sources are centered with the GPD. As a matter of fact, after the integration and in orbit deployment of mirrors, the focalized source beam could impinge on a different position, so that the observatory can dithers on a different portion of the GPD surface with respect to the one used for calibration. In this section the spatial uniformity of the polarimetric response is investigated. These studies will allow us to assess whether the results obtained in the central DFF region are valid for the whole GPD surface.

To verify the spatial uniformity of the response to polarized radiation of the DUs, we performed an analysis on the FF data sets at different energies, selecting 9 smaller, independent, regions with radius 2 mm (see Figure 5).

In these regions the modulation factor has been evaluated and the results allowed us to verify that the response of each DU is uniform on the whole sensitive area for each energy. For example, in Figure 6 the measured modulation factors in the nine regions for all the DUs are shown for the measurements at

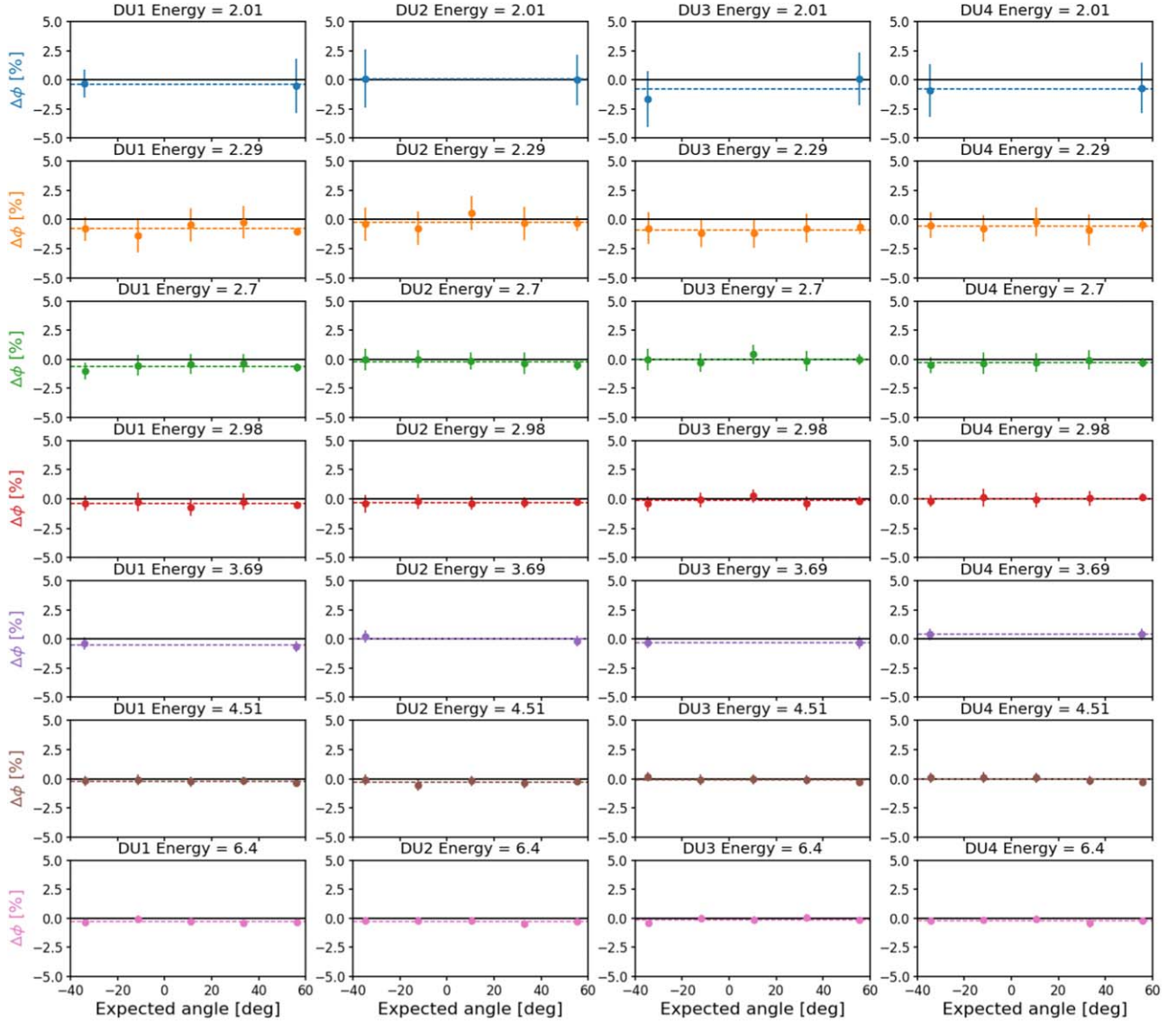


Figure 9. Deviation from the expected phase for polarization angle for each DU and energy. Data points are fitted with a constant line (dashed line).

2.98 keV and are compatible with a constant function. For each position, we can estimate $(\mu_i - \mu_0)/\sigma_{\mu_i}$, which is the number of standard deviations (σ_{μ_i}) between the measured modulation factor μ_i and the mean value (μ_0) obtained fitting each data set. The distribution of these values considering all the DUs and energies is shown in Figure 7 and it is possible to observe that the distribution is normally distributed around zero.

4.2. Dependence of Modulation Factor on the Polarization Angle

On the IXPE focal plane, the three DUs will be clocked at 120° one with respect to the other, which means that the DUs will measure three values of the polarization angle of an astrophysical source shifted by 120° with respect to the detector coordinates. Such configuration allows for checking the genuine polarization from celestial sources. If the spurious modulation is properly removed, we expect that the modulation factor is independent of the polarization angle. Indeed the possible presence of an additional $\cos^2 \phi$ spurious modulation contribution could modify the amplitude and phase of the

modulation curve from a polarized source, hence the measurement of the modulation factor. In this section, we study the modulation factor as a function of the polarization angles. Results are shown in Figure 8 for the four DUs at all the energies.

From this analysis results that the modulation factor does not depend on the polarization angle in the GPD frame once the spurious modulation is properly subtracted.

4.3. Absolute Knowledge of Polarization Angle

It is important for IXPE to determine precisely the polarization angle of a celestial source. This is because the polarization angle is correlated to the intrinsic geometry of the system under study and to the configuration of magnetic fields, such as in extended sources like supernova remnants and pulsar wind nebulae. A good knowledge of the position angle allows for comparing multiwavelength observations and detect secular variations. We recall that, at the level of the observatory, the knowledge of the position angle is 1 degree Soffitta et al. (2021). Therefore, it is necessary to determine the polarization

Table 3

Systematic Difference Between the Measured Polarization Angle and the Expected One from the Geometry of the Experimental Setup for Each IXPE DU-FM at Every Calibration Energy

Energy (keV)	DU-FM1 $\Delta\phi$ (deg)	DU-FM2 $\Delta\phi$ (deg)	DU-FM3 $\Delta\phi$ (deg)	DU-FM4 $\Delta\phi$ (deg)
2.01	-0.423 ± 0.073	0.047 ± 0.032	-0.79 ± 0.61	-0.802 ± 0.074
2.29	-0.78 ± 0.18	-0.24 ± 0.20	-0.90 ± 0.11	-0.56 ± 0.11
2.70	-0.60 ± 0.10	-0.201 ± 0.087	-0.03 ± 0.11	-0.293 ± 0.066
2.98	-0.427 ± 0.079	-0.320 ± 0.032	-0.16 ± 0.11	0.006 ± 0.053
3.69	-0.518 ± 0.092	0.03 ± 0.13	-0.3053 ± 0.0051	0.3860 ± 0.0010
4.51	-0.211 ± 0.041	-0.292 ± 0.078	-0.074 ± 0.067	-0.032 ± 0.066
6.40	-0.288 ± 0.046	-0.269 ± 0.049	-0.129 ± 0.070	-0.209 ± 0.055

Note. The values at 6.4 keV have to be compared with the scientific requirement of IXPE, which is 0.4° . These values and errors are obtained from the linear fits of Figure 9.

angle measurement accuracy with respect to the detector mechanical coordinates. For this reason, we used an Absolute Rohmer Arm with an accuracy of $\simeq 10 \mu\text{m}$, to map the geometry of the setup and to correlate the measured polarization angle with the one expected from this mechanical setup. In this analysis, we estimated the polarization angle by the data, then its expected value was subtracted. Results from this analysis are shown in Figure 9 for all the DUs and energies. In each box, points in color are the measured values fitted with a constant function (dashed line), to verify the ideal case (null hypothesis).

For all the energies and DUs from the fit with a constant value, an uncertainty on the polarization angle estimate has been determined. In particular at 6.4 keV the scientific requirement for IXPE, which is 0.4° , is reached for all the DUs (see Table 3). These values state the level of accuracy that IXPE can reach for the polarization angle at each energy in each DU.

4.4. Modulation Factor and Angle Systematic as a Function of Energy

The mean modulation factor estimated in Section 4.2 is plotted as a function of the energy for all the IXPE DUs in Figure 10—top, where data points are fitted with a quadratic spline. In Figure 10, bottom, the polarization angle uncertainty estimated in Section 4.3 is also reported as a function of the energy; the estimated values are reported in Table 3.

Scientific requirements are reported on the plot of Figure 10 and are satisfied for all DUs. The modulation factor values have been evaluated also using the unweighted approach of Kislat et al. (2015) and the “standard cuts” analysis, as shown in Table 4.

The modulation factor values and angle systematics for each DU are within the scientific requirement. The former is slightly different for the different DUs due to the small differences in the detectors (Baldini et al. 2021), which are accounted for in the generation of the response matrices.

4.5. Polarization Response for Off-axis Beams

Photons focused by a mirror are incident on the detector at an angle of the order of a few degrees. In the case of the GPD, this causes a systematic effect as expected and computed in Muleri (2014). Albeit the effect is anticipated to be small, we verified such an expectation by measuring the modulation

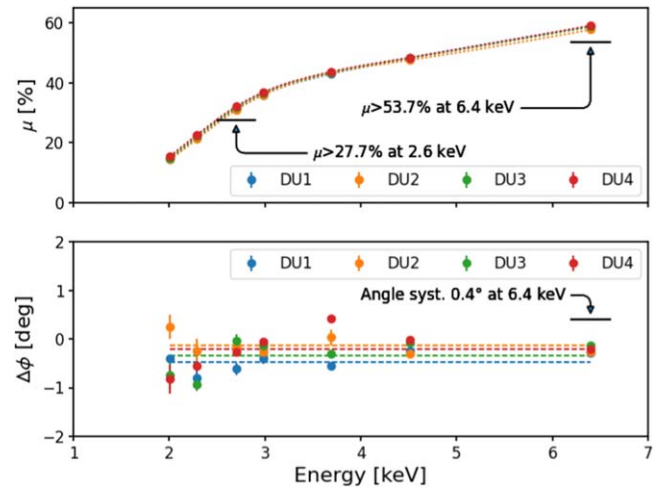


Figure 10. Modulation factor (top) and polarization angle systematic (bottom) as a function of energy. IXPE scientific requirements are reported in black. Mean values for the polarization angle systematic for each DU is reported as a dashed line.

factor at 2.7 keV for a beam which is inclined of $\pm 2^\circ$ with respect to both axes normal the focusing GPD window. This is the typical incidence angle from a focusing X-ray beam. Measurement is repeated at four azimuthal angles to simulate the focusing from an IXPE mirror. The modulation factors for the four angles are shown in Figure 11. As expected, the modulation factors do not change with the azimuthal angle and the overall inclined modulation factor is compatible with the noninclined one.

The modulation factors are constant within the uncertainties.

5. Conclusions

Since IXPE is a discovery mission, known calibrated celestial sources are not available for performing in-flight calibration for polarimetry. In fact, the measurement performed 45 yr ago on the Crab Nebula (Weisskopf et al. 1976, 1978) and the recent ones by PolarLight (Feng et al. 2020; Long et al. 2022) cannot be used as a flight calibrator. Moreover, these missions were not imaging, for these reasons a detailed ground calibration was mandatory.

At this aim, a wide calibration campaign was performed at INAF-IAPS. During the campaign, data were acquired 24 hr

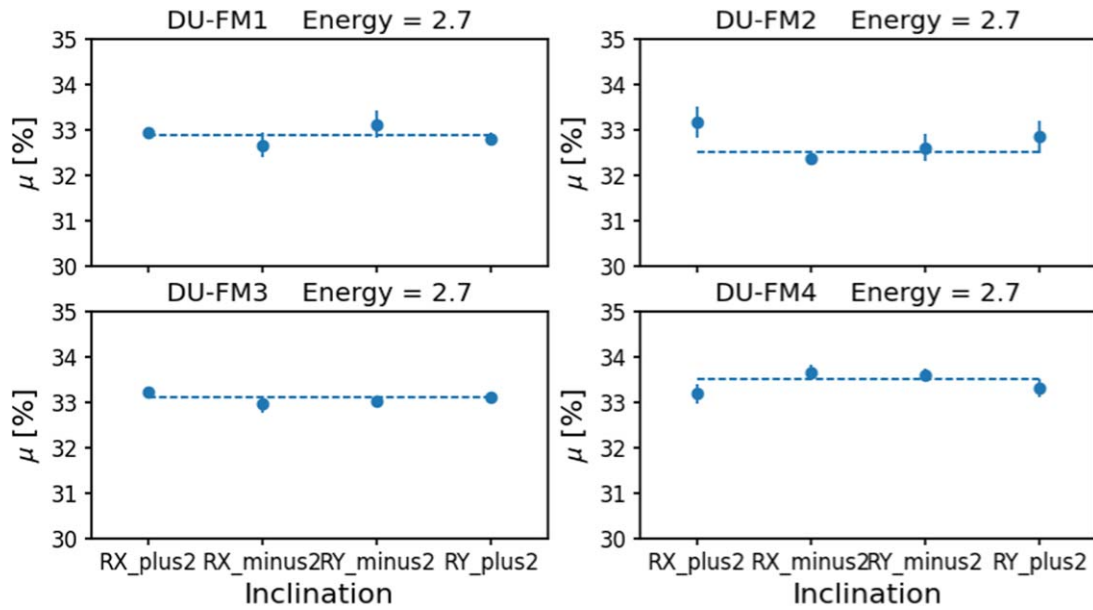


Figure 11. Modulation factor for the inclined measurements at 2.7 keV. They are compatible with a constant as expected.

Table 4

Modulation Factor Evaluated with the Weighted Analysis of Di Marco et al. (2022), the Unweighted One of Kislat et al. (2015), and the “Standard Cuts”

Weighted Analysis				
Energy [keV]	DU-FM1 μ [%]	DU-FM2 μ [%]	DU-FM3 μ [%]	DU-FM4 μ [%]
2.01	14.653 ± 0.048	14.4060 ± 0.0057	14.99 ± 0.14	15.557 ± 0.019
2.29	21.567 ± 0.059	21.262 ± 0.067	22.182 ± 0.054	22.64 ± 0.16
2.70	31.291 ± 0.045	30.949 ± 0.098	31.810 ± 0.086	32.128 ± 0.084
2.98	36.028 ± 0.082	35.858 ± 0.088	36.55 ± 0.10	36.769 ± 0.057
3.69	42.97 ± 0.35	43.19 ± 0.10	43.437 ± 0.093	43.66 ± 0.13
4.51	48.26 ± 0.11	47.581 ± 0.085	48.229 ± 0.067	48.40 ± 0.12
6.40	58.796 ± 0.042	57.729 ± 0.042	58.660 ± 0.094	59.103 ± 0.089
Unweighted analysis				
Energy [keV]	DU-FM1 μ [%]	DU-FM2 μ [%]	DU-FM3 μ [%]	DU-FM4 μ [%]
2.01	12.644 ± 0.029	12.406 ± 0.092	12.827 ± 0.065	13.405 ± 0.040
2.29	18.054 ± 0.044	17.803 ± 0.055	18.563 ± 0.088	18.960 ± 0.092
2.70	25.817 ± 0.032	25.547 ± 0.066	26.169 ± 0.071	26.60 ± 0.10
2.98	30.049 ± 0.064	29.877 ± 0.094	30.422 ± 0.076	30.771 ± 0.038
3.69	36.99 ± 0.30	37.183 ± 0.096	37.37 ± 0.12	37.73 ± 0.18
4.51	42.787 ± 0.097	42.165 ± 0.060	42.770 ± 0.054	42.98 ± 0.13
6.40	54.614 ± 0.061	53.418 ± 0.060	54.46 ± 0.11	54.889 ± 0.081
Standard cuts analysis				
Energy [keV]	DU-FM1	DU-FM2	DU-FM3	DU-FM4
2.01	12.94 ± 0.12	12.68 ± 0.13	12.901 ± 0.098	13.653 ± 0.014
2.29	20.582 ± 0.062	20.318 ± 0.072	21.221 ± 0.075	21.62 ± 0.18
2.70	29.447 ± 0.036	29.156 ± 0.064	29.916 ± 0.088	30.348 ± 0.098
2.98	34.099 ± 0.081	33.905 ± 0.090	34.466 ± 0.087	34.834 ± 0.065
3.69	40.97 ± 0.39	41.23 ± 0.13	41.31 ± 0.18	41.60 ± 0.14
4.51	46.38 ± 0.12	45.763 ± 0.078	46.236 ± 0.046	46.47 ± 0.13
6.40	56.624 ± 0.044	55.987 ± 0.068	56.392 ± 0.062	56.89 ± 0.14

Note. The best value is obtained using the weighted analysis.

per day and 7 days per week; for each DU, at least 40 days of calibrations were needed. At the end of these calibrations, the results of this article were obtained for the IXPE polarimetric response, in particular:

1. polarimetric response is uniform on the detector surface, once that spurious modulation has been subtracted;
2. scientific requirements on the modulation factor at 2.6 and 6.4 keV are satisfied;














3. once the response to unpolarized radiation is calibrated, the modulation factor is constant with the polarization angle;
4. systematic error on polarization angle at 6.4 keV does not exceed 0.4°;
5. modulation factor does not depend on the X-ray beam inclination, thus it will be not affected by effects due to inclined penetration from the mirrors.

As a matter of fact, IXPE is equipped with both polarized and unpolarized sources to be used for checking the stability of the instrument's response during operation (Ferrazzoli et al. 2020). The response to polarized sources has been measured estimated with different analysis approaches that have been reported in Table 4. It is possible to observe that the weighted analysis of Di Marco et al. (2022) allows for obtaining the highest value of modulation factor. These results are used as a reference to obtain the IXPE CALDB distributed on HEASARC with the detectors response functions.

The Italian contribution to the IXPE mission is supported by the Italian Space Agency (ASI) through the contract ASI-OHBI-2017-12-I.0, the agreements ASI-INAF-2017-12-H0 and ASI-INFN-2017.13-H0, its Space Science Data Center (SSDC), by the Istituto Nazionale di Astrofisica (INAF), and the Istituto Nazionale di Fisica Nucleare (INFN) in Italy.

IXPE is a NASA Astrophysics Small Explorers (SMEX) mission, managed by MSFC and overseen by the Explorers Program Office at GSFC.

ORCID iDs

Alessandro Di Marco  <https://orcid.org/0000-0003-0331-3259>
 Sergio Fabiani  <https://orcid.org/0000-0003-1533-0283>
 Fabio La Monaca  <https://orcid.org/0000-0001-8916-4156>
 Fabio Muleri  <https://orcid.org/0000-0003-3331-3794>
 John Rankin  <https://orcid.org/0000-0002-9774-0560>
 Paolo Soffitta  <https://orcid.org/0000-0002-7781-4104>
 Fabrizio Amici  <https://orcid.org/0000-0002-2637-8971>
 Matteo Bachetti  <https://orcid.org/0000-0002-4576-9337>
 Luca Baldini  <https://orcid.org/0000-0002-9785-7726>
 Ronaldo Bellazzini  <https://orcid.org/0000-0002-2469-7063>
 Rita Carpentiero  <https://orcid.org/0000-0002-7723-8135>
 Marco Castronuovo  <https://orcid.org/0000-0002-6103-332X>
 Elisabetta Cavazzuti  <https://orcid.org/0000-0001-7150-9638>

Enrico Costa  <https://orcid.org/0000-0003-4925-8523>
 Ettore Del Monte  <https://orcid.org/0000-0002-3013-6334>
 Riccardo Ferrazzoli  <https://orcid.org/0000-0003-1074-8605>
 Luca Latronico  <https://orcid.org/0000-0002-0984-1856>
 Simone Maldera  <https://orcid.org/0000-0002-0698-4421>
 Alberto Manfreda  <https://orcid.org/0000-0002-0998-4953>
 Giorgio Matt  <https://orcid.org/0000-0002-2152-0916>
 Alessio Nuti  <https://orcid.org/0000-0002-9352-2355>
 Matteo Perri  <https://orcid.org/0000-0003-3613-4409>
 Melissa Pesce-Rollins  <https://orcid.org/0000-0003-1790-8018>
 Raffaele Piazzolla  <https://orcid.org/0000-0002-4222-6919>
 Maura Pilia  <https://orcid.org/0000-0001-7397-8091>
 Simonetta Puccetti  <https://orcid.org/0000-0002-2734-7835>
 Carmelo Sgrò  <https://orcid.org/0000-0001-5676-6214>
 Martin C. Weisskopf  <https://orcid.org/0000-0002-5270-4240>

References

- Baldini, L., Barbanera, M., Bellazzini, R., et al. 2021, *APh*, 133, 102628
 Barbanera, M., Citraro, S., Magazzù, C., et al. 2021, *ITNS*, 68, 1144
 Bellazzini, R., Spandre, G., Minuti, M., et al. 2006, *NIMPA*, 566, 552
 Bellazzini, R., Spandre, G., Minuti, M., et al. 2007, *NIMPA*, 579, 853
 Bongiorno, S. D., Kolodziejczak, J. J., Kilaru, K., et al. 2021, *Proc. SPIE*, 11822, 189
 Costa, E., Soffitta, P., Bellazzini, R., et al. 2001, *Natur*, 411, 662
 Di Marco, A., Costa, E., Muleri, F., et al. 2022, *AJ*, 163, 170
 Ferrazzoli, R., Muleri, F., Lefevre, C., et al. 2020, *JATIS*, 6, 048002
 Heitler, W. 1936, *The Quantum Theory of Radiation* (International Series of Monographs on Physics Vol. 5) (Oxford: Oxford Univ. Press)
 Kislak, F., Clark, B., Beilicke, M., & Krawczynski, H. 2015, *Aph*, 68, 45
 La Monaca, F., Fabiani, S., Lefevre, C., et al. 2021, *Proc. SPIE*, 11444, 1029
 Long, X., Feng, H., Li, H., et al. 2022, *ApJL*, 924, L13
 Muleri, F. 2014, *ApJ*, 782, 28
 Muleri, F., Soffitta, P., Baldini, L., et al. 2016, *Proc. SPIE*, 9905, 1401
 Muleri, F., Lefevre, C., Piazzolla, R., et al. 2018, *Proc. SPIE*, 10699, 1312
 Muleri, F., Piazzolla, R., Di Marco, A., et al. 2021, *Aph*, 136, 102658
 O'Dell, S. L., Attinà, P., Baldini, L., et al. 2019, *Proc. SPIE*, 11118, 248
 Ramsey, B. D., Attina, P., Baldini, L., et al. 2021, *Proc. SPIE*, 11821, 225
 Rankin, J., Muleri, F., Tennant, A. F., et al. 2022, *AJ*, 163, 39
 Sgrò, C. 2017, *Proc. SPIE*, 10397, 104
 Soffitta, P. 2017, *Proc. SPIE*, 10397, 127
 Soffitta, P., Attinà, P., Baldini, L., et al. 2020, *Proc. SPIE*, 11444, 1017
 Soffitta, P., Baldini, L., Bellazzini, R., et al. 2021, *AJ*, 162, 208
 Strohmayer, T. E., & Kallman, T. R. 2013, *ApJ*, 773, 103
 Weisskopf, M. C., Cohen, G. G., Kestenbaum, H. L., et al. 1976, *ApJL*, 208, L125
 Weisskopf, M. C., Silver, E. H., Kestenbaum, H. L., Long, K. S., & Novick, R. 1978, *ApJL*, 220, L117
 Weisskopf, M. C., Ramsey, B., O'Dell, S., et al. 2016, *Proc. SPIE*, 9905, 356
 Weisskopf, M. C., Soffitta, P., Baldini, L., et al. 2021, *JATIS*, 8, 1